



Reduction of Eu^{3+} to Eu^{2+} in $\text{NaCaPO}_4:\text{Eu}$ phosphors prepared in a non-reducing atmosphere

Bhaskar Kumar Grandhe^a, Vengala Rao Bandi^a, Kiwan Jang^{a,*}, Sang-Su Kim^a, Dong-Soo Shin^b, Yong-Ill Lee^b, Jae-Min Lim^b, Taekwon Song^c

^a Department of Physics, Changwon National University, Changwon 641773, Republic of Korea

^b Department of Chemistry, Changwon National University, Changwon 641773, Republic of Korea

^c School of Nano and Advanced Materials Engineering, Changwon National University, Changwon 641773, Republic of Korea

ARTICLE INFO

Article history:

Received 19 April 2011

Received in revised form 7 May 2011

Accepted 12 May 2011

Available online 19 May 2011

Keywords:

Phosphate phosphors

Europium

Reduction

Non-reducing atmosphere

ABSTRACT

The reduction of Eu^{3+} to Eu^{2+} in a non-reducing atmosphere of pure argon gas has been reported for the first time in NaCaPO_4 host matrix prepared by using a solid-state reaction. Photoluminescence spectral profiles confirmed the presence of Eu^{2+} ions in the prepared compound and this reduction has been explained by means of a charge compensation model. The effect of lithium incorporation on the photoluminescence efficiency of the $\text{NaCaPO}_4:\text{Eu}^{2+}$ phosphors were also studied and explained appropriately for various doping concentrations of lithium ions. The CIE coordinates and temperature dependant luminescence profiles of these phosphors were also discussed in order to investigate their potential applications. Besides analyzing its photoluminescence properties, other significant characterizations like XRD, SEM, TG–DTA, FTIR, Raman spectral profiles have also been studied and these interpretations were documented more clearly.

© 2011 Elsevier B.V. All rights reserved.

1. Introduction

Over the last few decades, optical properties of rare-earth (RE) ions doped into various host materials have been studied extensively, mainly with respect to their potential applications in solid state lighting, displays, lasers, optical amplifiers, sensors, etc. Of the various RE elements, europium ion plays a dominant role. Europium ions are widely selected and used as activators in commercial phosphors, such as $\text{Y}_2\text{O}_3:\text{Eu}^{3+}$ and $\text{BaMgAl}_{10}\text{O}_{17}:\text{Eu}^{2+}$ with two normal valence states, viz. +2 and +3. Drastic spectral changes are associated with the change in oxidation state of the rare earths. As usual, Eu^{3+} , which is stable under ambient conditions, exhibits the line emission features due to the forbidden f–f transitions (located in 550–750 nm); while the divalent europium ion, which is sensitive to oxygen and therefore unstable in air, shows the narrow-band and broad-band emissions due to their f–f transitions (lying around 360 nm) and f–d transitions (not lying in a definite wavelength but strongly depending on hosts) respectively [1–4].

Inorganic luminescent materials, especially activated by divalent europium ions (Eu^{2+}), have been widely used in modern lighting, displays and optical communications fields such as fluorescent lamps, cathode ray tubes, field emission displays, plasma

display panels and fiber amplifier [4]. Since the divalent Eu^{2+} ions exist under a limited condition, no Eu^{2+} ion containing compound could be obtained as a natural product. Therefore, the starting material of the europium compound in preparing luminescent materials is always trivalent europium oxide (Eu_2O_3). In the reduction processes of Eu^{3+} to Eu^{2+} , the four different cases which attract the researchers attention are (a) the reduction is completely achieved when samples are prepared in a reducing atmosphere (H_2 – N_2 or CO); (b) this reduction could not be completely realized when samples are synthesized in a reducing environment; (c) it is impossible to obtain Eu^{2+} ions even if the preparation is carried out in a strong reducing atmosphere and (d) in some special hosts, this reduction can be realized even when samples are prepared in non-reducing atmosphere (air, N_2 and Ar). For environmental and technological reasons, (d) is encouraging, but can be applied only to a limited number of systems [5–7].

NaCaPO_4 host matrix has lower synthesis temperature and higher physical and chemical stability, which makes it as a suitable host lattice for luminescence materials [8]. It also possesses an appropriate structure containing a rigid three-dimensional network of tetragonal PO_4 groups. These groups can surround and isolate the produced divalent RE ions from the reaction with oxygen. Therefore, this reduction reaction can be carried out even in a non-reducing atmosphere [5,9]. In the present article, we report the reduction phenomenon of Eu^{3+} ions to Eu^{2+} ions in $\text{NaCaPO}_4:\text{Eu}$ phosphor prepared by a conventional solid state reaction method in

* Corresponding author. Tel.: +82 55 213 3425; fax: +82 55 267 0263.

E-mail address: kwjang@changwon.ac.kr (K. Jang).

a non-reducing atmosphere of pure argon gas. As far as our knowledge is concerned, this type of reduction in the case of NaCaPO_4 host matrix has not been reported so far. In addition, its structural, thermal, optical, photoluminescence properties along with the temperature dependant luminescent behavior were also studied and analyzed.

2. Experimental

Europium ions doped NaCaPO_4 phosphors were prepared by a conventional solid state reaction method by sintering the sample at 850°C in pure argon atmosphere. The optimized doping concentration of europium ion in NaCaPO_4 phosphors was found to be 1.0 mol% of the Ca ion of NaCaPO_4 phosphors. Analytical reagent grade high pure Na_2CO_3 , Li_2CO_3 , CaCO_3 , $\text{NH}_4\text{H}_2\text{PO}_4$ and Eu_2O_3 chemicals were weighed in requisite proportions and grounded in an agate mortar with methyl alcohol to obtain homogeneous mixture. Differential thermal analysis (DTA) and thermo gravimetric analysis were employed to determine the suitable heat treatment procedure. The mixture was kept in an alumina crucible and sintered in pure argon atmosphere by a three-step heating process (200°C for 2 h, 700°C for 1 h, and 850°C for 3 h) to obtain $\text{Eu}^{2+}:\text{NaCaPO}_4$ phosphor.

The crystal structure of the prepared phosphors was investigated by using X-ray powder diffraction (Philips X'pert, MPD 3040, Westborough, MA) over the 2θ range from 20° to 60° . The morphology of the powder phosphors was observed by employing field emission-scanning electron microscope (FE-SEM) (Tescan, MIRA IILMH, Brno, Czech Republic). FTIR spectrum of the phosphor sample was recorded on a Jasco FTIR-200 E spectrometer with KBr pellet technique from 4000 cm^{-1} to 400 cm^{-1} . Raman spectrum was recorded by using a high resolution NRS-3300 laser Raman spectrophotometer (JASCO) system equipped with a DPSS green diode laser (532 nm) as the excitation source. Emission and excitation spectra were measured using a Shimadzu, RF-5301PC spectro- fluorophotometer (Kyoto, Japan). The TG-DTA analysis were performed by using the thermal analyzer system (Model: TA 5000/SDT 2960 DSC Q10) in a alumina crucible at heating rate $10^\circ\text{C}/\text{min}$, from 20°C to 1000°C at N_2 gas atmosphere. To measure temperature dependent relative emission intensity, a continuous wave (CW) xenon lamp (Thermo Oriol Instruments) was used as excitation source and PL spectra were measured by a USB spectrometer (Ocean Optics Model the USB2000 spectrometer). All spectroscopic measurements were performed at room temperature.

3. Results and discussion

Fig. 1 shows the XRD patterns of $\text{NaCa}_{0.99}\text{PO}_4:\text{Eu}_{0.01}$ and $\text{Na}_{0.96}\text{Li}_{0.04}\text{Ca}_{0.99}\text{PO}_4:\text{Eu}_{0.01}$ phosphors sintered in pure argon atmosphere. It reveals that the XRD patterns of these optimized phosphor samples are in good agreement with the Joint Committee on Powder Diffraction Standards (JCPDS) data card bearing the number 29-1193, indicating that the incorporated dopant ions have not caused any significant changes to the orthorhombic crys-

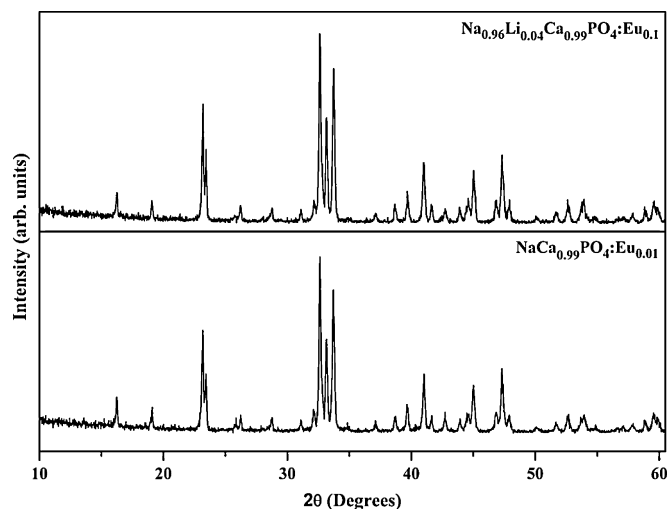


Fig. 1. XRD profiles of $\text{Na}_{1-x}\text{Li}_x\text{Ca}_{1-y}\text{PO}_4:\text{Eu}_y$ phosphors sintered in argon atmosphere.

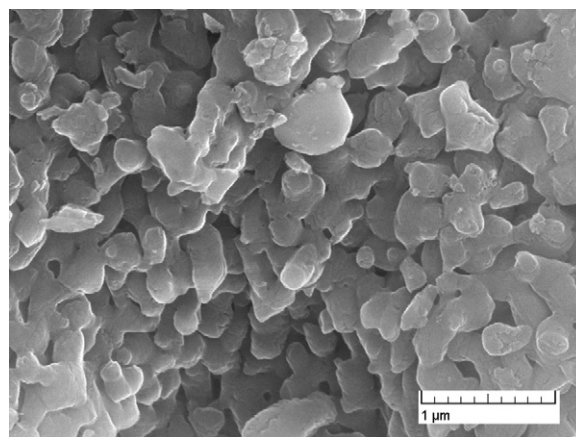


Fig. 2. FE-SEM image of $\text{NaCa}_{0.99}\text{PO}_4:\text{Eu}_{0.01}$ phosphors sintered in argon atmosphere.

tal structure of NaCaPO_4 matrix. The average crystallite size was estimated by using Scherrer equation

$$D_{hkl} = \frac{k\lambda}{\beta(2\theta)\cos\theta}$$

where $\beta(2\theta)$ is the width of the pure diffraction profile in radians, k is the constant, λ is the wavelength of the X-rays (0.15406 nm), θ is the diffraction angle and D_{hkl} is the average crystallite size along (hkl) direction. By fitting various peaks to this formula and taking into account the instrumental broadening, we found that the mean crystallite size of the phosphor particles are in the range of $137\text{--}144\text{ nm}$ for $\text{NaCa}_{0.99}\text{PO}_4:\text{Eu}_{0.01}$ phosphors and $\text{Na}_{0.96}\text{Li}_{0.04}\text{Ca}_{0.99}\text{PO}_4:\text{Eu}_{0.01}$ phosphors, respectively. FE-SEM image of $\text{NaCa}_{0.99}\text{PO}_4:\text{Eu}_{0.01}$ phosphors sintered in argon atmosphere calcined at 850°C is presented in Fig. 2. The obtained micrograph shows that the particles are agglomerated and it possesses an irregular morphology. For this reason, accurate measurement of particle size might not be possible from it. The approximate size of those particles might be in micrometer range which is a suitable size for fabrication of SSL devices. From literature, it is noticed that the crystalline powder in micrometer dimension will find more applications as it can exhibit high luminescent intensities [10].

FTIR spectrum of the Eu^{2+} ions doped $\text{NaCa}_{0.99}\text{PO}_4:\text{Eu}_{0.01}$ phosphor sintered in argon atmosphere is shown in Fig. 3(a). Usually, the

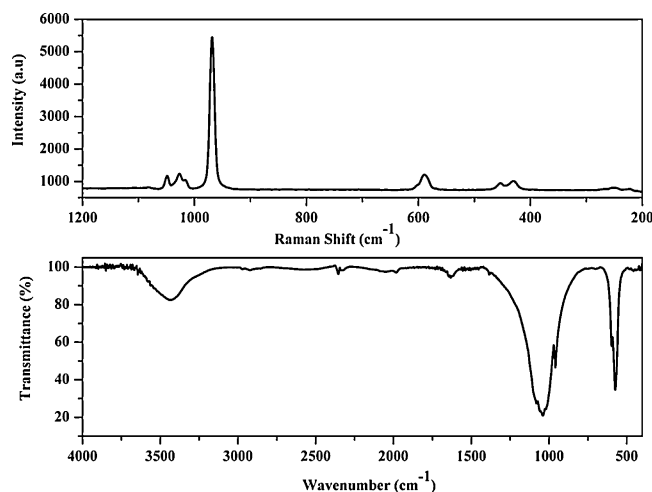


Fig. 3. (a) FTIR spectrum and (b) Raman spectrum of $\text{NaCa}_{0.99}\text{PO}_4:\text{Eu}_{0.01}$ phosphors sintered in argon atmosphere.

IR absorption band of $(\text{PO}_4)^{3-}$ has two regions of $1120\text{--}940\text{ cm}^{-1}$ and $650\text{--}540\text{ cm}^{-1}$. The phosphate units in Fig. 3(a) are characterized by two broad IR absorption bands centered near 1050 and 570 cm^{-1} are assigned to the symmetric stretching mode of the $(\text{PO}_4)^{3-}$ units. However, we noticed some insignificant bands near 1636 cm^{-1} and 3440 cm^{-1} that are associated to the OH content absorbed at the powder surface when the sample was in contact with the environment during the preparation process of measurement [11–14]. Fig. 3(b) shows the Raman spectrum of $\text{NaCa}_{0.99}\text{PO}_4:\text{Eu}_{0.01}$ phosphors sintered in argon atmosphere. The basic vibration modes from $(\text{PO}_4)^{3-}$ free ions have four modes: $\nu_1(\text{A}_1)$ of P–O symmetric stretching vibration, $\nu_2(\text{E})$ of PO_2 symmetric bending vibration, $\nu_3(\text{F}_2)$ of PO asymmetric stretching vibration and $\nu_4(\text{F}_2)$ of PO_2 asymmetric bending vibration in the $(\text{PO}_4)^{3-}$ tetrahedron. In the crystal structure, $(\text{PO}_4)^{3-}$ vibration may have some changes due to disorder of the local point symmetry and anion O_2^- ions. The band at 967 cm^{-1} is assigned to $\nu_1(\text{PO}_4)^{3-}$ symmetric stretching vibration, 429 cm^{-1} and 454 cm^{-1} to $\nu_2(\text{PO}_4)^{3-}$ bending vibrations, 1048 and 1027 cm^{-1} to $\nu_3(\text{PO}_4)^{3-}$ antisymmetric stretching vibrations and 591 cm^{-1} to $\nu_4(\text{PO}_4)^{3-}$ bending vibration, respectively. All the assignments made above are in good agreement with the earlier literature reports [13–15].

The TG–DTA profile of $\text{NaCa}_{0.99}\text{PO}_4:\text{Eu}_{0.01}$ phosphor precursor is shown in Fig. 4. In the temperature range from 20°C to 200°C , the sample shows both exothermic and endothermic peaks in the DTA curve, which is consistent with the first weight loss. These observations can be attributed to the decomposition of NH_3 , H_2O and the organic species used during the grinding process. The second weight loss in the range of $200\text{--}700^\circ\text{C}$ is due to the degradation of any other residual organic material from the precursor which is also accompanied by the removal of CO_2 gases that occurs from the starting chemicals. Upon increasing the temperature a solid state reaction occurs among those precursor chemicals and peaks observed in the DTA curve confirm such reaction. TG curve indicates a total weight loss of nearly 38% when the temperature is raised from 30°C to 1000°C . No significant weight loss has been observed in the TG curve when the temperature is raised beyond 800°C .

The luminescent properties of the optical materials are closely correlated with the valence state of the activator ions. As is well known, some kinds of reducing agents, such as H_2/CO , are needed to reduce the Eu^{3+} to Eu^{2+} in a solid state compound. But in some special cases, this reduction could be thermally achieved in a non-reducing atmosphere at high temperatures as in air/ N_2/Ar . When phosphors are prepared by conventional solid-state route by heating in air, usually unwanted impurities like OH^- , O^{2-} , etc., get

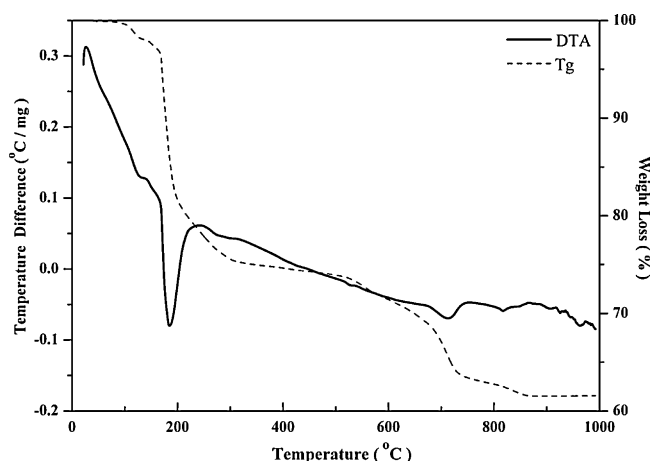


Fig. 4. TG–DTA profile of $\text{NaCa}_{0.99}\text{PO}_4:\text{Eu}_{0.01}$ phosphor precursor.

incorporated. Such impurities can be quite harmful to the luminescence processes [16]. Fig. 5(a) shows the excitation spectra of $\text{NaCaPO}_4:\text{Eu}^{2+}$ phosphor sintered in pure argon atmosphere, monitored at 505 nm , showing a broad band, which extends from 250 to 450 nm . This intense band can be attributed to the $4f\text{--}5d$ transition of Eu^{2+} ions [17]. The prominent excitation peak is located at 373 nm , which indicates that the phosphor is very suitable for a color converter using UV light as the primary light source. It can be used as a green phosphor excited by UV LED chip and mixed with other color emission phosphors to obtain white light. Fig. 5(b) shows the emission spectra of $\text{NaCaPO}_4:\text{Eu}^{2+}$ phosphors sintered in pure argon atmosphere and measured 373 nm as the excitation wavelength. The emission spectra are dominated by the broad and intense band at 505 nm , which is ascribed to the $4f^65d \rightarrow 4f^7(^8S_{7/2})$ transition on Eu^{2+} ions [17,18]. It corresponds to the allowed f–d transition of Eu^{2+} . The $5d$ energy level of Eu^{2+} and the lower level of $4f$ state overlap, so the electron of $4f$ state can be excited to $5d$ state. The broad luminescence of Eu^{2+} is due to $4f^65d_1 \rightarrow 4f_7$ transitions, which is an allowed electrostatic dipole transition. However, the $5d$ state is easily affected by the crystal field; that is to say, different crystal fields can split the $5d$ state in a different way. This makes Eu^{2+} ion emitting different wavelengths in different crystal fields and the emission spectrum can vary from the ultraviolet to the red region. Covalence, the size of the cation, and the strength of the crystal field influence Eu^{2+} ions emission color [17,19]. It can be concluded that Eu^{2+} ion exists and the reduction of Eu^{3+} to Eu^{2+} occurs in $\text{NaCaPO}_4:\text{Eu}$ phosphors prepared in a non-reducing atmosphere of pure argon gas. The full width at half maximum (FWHM) of the emission band is around 76 nm .

The inset of Fig. 5 shows the graph between emission intensity and Eu^{2+} dopant concentration. It is evident from figure that the $1.0\text{ mol}\%$ doped NaCaPO_4 phosphor sample display better emission profile than the other concentration samples. The positions of the emission peak are not much influenced by the Eu^{2+} concentration. The emission intensity increases with increasing of Eu^{2+} concentration, and reaches the maximum at about $1.0\text{ mol}\%$. Concentration quenching occurs, when the Eu^{2+} concentration is beyond $1.0\text{ mol}\%$. Qiu et al. [20] showed that the probability of energy transfer among the Eu^{2+} ions increases to a certain extent with the increase in Eu^{2+} ion concentration in the host matrix. The energy transfer occurred between the Eu^{2+} ions in $\text{NaCaPO}_4:\text{Eu}^{2+}$ phosphor is due to electric multipole–multipole interaction [18]. Intense green emission for 373 nm excitation wavelength indicates that $\text{NaCaPO}_4:\text{Eu}^{2+}$ can be potentially used as a green phosphor in near-UV LEDs.

According to earlier published reports, there are four conditions that are necessary to reduce Eu^{3+} to Eu^{2+} in solid state compounds when prepared in non-reducing atmosphere [6,21]. These are as follows: (a) no oxidizing ions are present in the host compounds; (b) the dopant trivalent Eu^{3+} ion replaces a divalent cation in the host; (c) the substituted cation has a similar radius to the divalent Eu^{2+} ion and (d) the host compound has an appropriate structure, based upon tetrahedral anion groups (BO_4 , SO_4 , PO_4 , or AlO_4). We will consider NaCaPO_4 based on the four conditions mentioned above. An acceptable percentage difference in ionic radii between doped and substituted ions must not exceed 30% [22]. The calculations of the radius percentage difference between the doped ions (Eu^{3+}) and the possible substituted ions (Ca^{2+} and P^{5+}) in NaCaPO_4 are analyzed based on the following equation:

$$\text{Dr} = 100 \times \frac{\text{Rm}(\text{CN}) - \text{Rd}(\text{CN})}{\text{Rm}(\text{CN})}$$

where Dr is the radius percentage difference, CN is the coordination number, Rm(CN) is the radius of the host cation, and Rd(CN) is the radius of doped ion. Taking the above formula into consideration and calculating those values for the possible substituted ions (Ca^{2+}

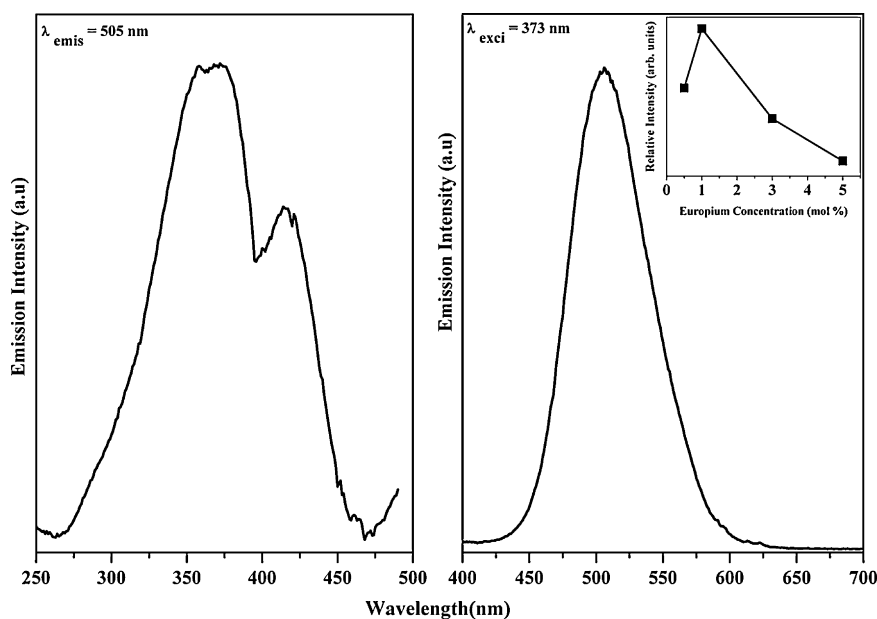


Fig. 5. PL excitation and emission spectra of $\text{NaCa}_{0.99}\text{PO}_4:\text{Eu}_{0.01}$ phosphors sintered in argon atmosphere. The inset shows the graph between emission intensity and dopant concentration.

and P^{5+}), the value of D_r between Eu^{3+} and Ca^{2+} on eight coordinated sites was found to be 4.8%, while the value of D_r between Eu^{3+} and P^{5+} is -457.05% . Hence it is interpreted that, europium ions has substituted the Ca^{2+} sites in NaCaPO_4 matrix. On the basis of the Shannon effective ionic radii of cations [23], it is clear that the Eu^{3+} (1.066 Å) ion prefer to substitute the Ca^{2+} (1.12 Å) ions because of their similar ionic radii. The above analysis showed that conditions (b) and (c) were satisfied. In NaCaPO_4 compound there exists no oxidizing ions, which satisfy condition (a). Besides, host compound has an appropriate structure, based upon tetrahedral anion groups (PO_4), as evident from obtained FTIR spectrum (Fig. 3) of the prepared sample and hence the condition (d) is also satisfied. Therefore, all the four conditions for the reduction of Eu^{3+} to Eu^{2+} in $\text{NaCaPO}_4:\text{Eu}$ prepared in non-reducing atmosphere condition are satisfied.

Further, the mechanism involved in the reduction of europium ions in the NaCaPO_4 matrix can be explained as follows: from a chemistry point of view, the reduction of Eu^{3+} to Eu^{2+} reaction needs an electron anyway. When trivalent Eu^{3+} ions are doped in to NaCaPO_4 matrix, they will replace the Ca^{2+} ions. To keep the electro neutrality of the compound, two Eu^{3+} ions would substitute for three Ca^{2+} ions. Therefore, two positive defects of $[\text{Eu}_{\text{Ca}}]^+$ and one negative Ca^{2+} vacancy of $[\text{V}_{\text{Ca}}]^-$ would be created by each substitution for every two Eu^{3+} ions in the compound. By thermal stimulation, electrons of the $[\text{V}_{\text{Ca}}]^-$ vacancies would be then transferred to doped Eu^{3+} ions and reduce them to Eu^{2+} ions. Hence it is assumed that the more electrons carried by negative defects were created; the more Eu^{3+} ions would be reduced to Eu^{2+} ions. Owing to these reasons of charge compensation, Eu^{3+} subsequently intrinsically reduced to Eu^{2+} . The rigid three-dimensional network of tetragonal PO_4 groups can surround and isolate the produced divalent europium ions from reacting with oxygen. Thus, necessary existence of defect electrons and the anion structures of compounds play an important role in the transfer process of defect electrons to the doped RE^{3+} ions by thermal stimulation [7,9].

The temperature-dependent luminescence spectrum for the observed intense green emission under an excitation of 373 nm is shown in Fig. 6. It can be seen that the $\text{NaCaPO}_4:\text{Eu}^{2+}$ phosphor displays an excellent thermal stability on the temperature quenching effect. It is an essential requirement that phosphors for

white LED applications should have low thermal quenching in order to avoid the changes in chromaticity and brightness of the white LEDs [24]. The residual emission intensity of Eu^{2+} doped NaCaPO_4 Phosphor at 250°C is still as high as 73.5% of the initial intensity at room temperature, whereas it is only 62% for a standard YAG:Ce (Daejoo electronic materials, Korea) phosphor. The comparison between the thermal stability of those phosphors is shown in the inset of Fig. 6. Such thermally stable NaCaPO_4 phosphor can serve better in improving the brightness of white-LEDs of high conversion efficiency at high junction temperatures. Although, YAG:Ce and $\text{NaCaPO}_4:\text{Eu}^{2+}$ phosphors are emitting yellow and green colors respectively, in our present study we have compared their thermal stabilities for reference purpose only.

From Fig. 6, we can also clearly notice a gradual decrease in the emission intensities as the temperature increases. This phenomenon can be described by thermal quenching in the configurational coordinate diagram [25]. The excited luminescent center is thermally activated through phonon interaction, and then ther-

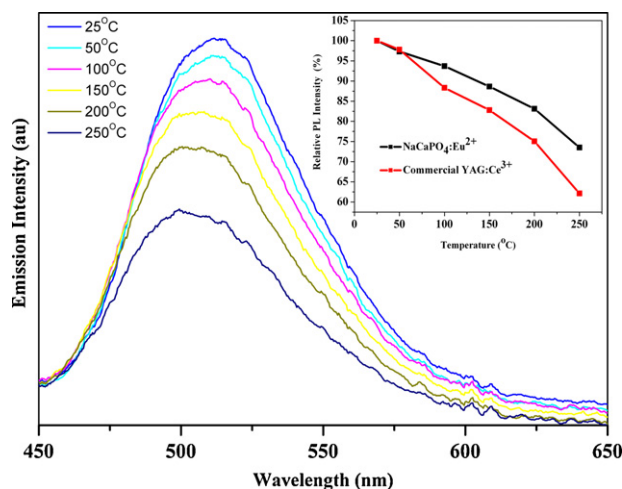


Fig. 6. Temperature dependent emission spectra of $\text{NaCa}_{0.99}\text{PO}_4:\text{Eu}_{0.01}^{2+}$ phosphors sintered in argon atmosphere. The inset shows the temperature-dependent relative emission intensities of the $\text{NaCa}_{0.99}\text{PO}_4:\text{Eu}_{0.01}^{2+}$ and YAG:Ce phosphors samples.

mally released through the crossing point between the excited state and the ground state in configurational coordinate diagram. This non-radiative transition probability by thermal activation is strongly dependent on temperature resulting in the decrease of emission intensity. The thermally activated luminescent center is strongly interacted with thermally active phonon, contributing to FWHM of emission spectrum. At higher temperature, the population density of phonon is increased, and the electron–phonon interaction is dominant, and consequently FWHM of emission spectrum is broadened [17,24].

Several groups have investigated the effect of lithium incorporation on the phosphor efficiency. Such studies revealed that the photoluminescent efficiency of many phosphors was enhanced remarkably by the incorporation of Li ions [26,27]. For this reason, in our present investigation we have also incorporated Li ions in place of Na ions to study its influence on the photoluminescence properties of the $\text{NaCaPO}_4:\text{Eu}^{2+}$ phosphor. We observed a drastic enhancement in the photoluminescence efficiency of $\text{NaCaPO}_4:\text{Eu}^{2+}$ phosphor when lithium ions are co doped. Fig. 7 reveals that among all the Li incorporated samples, the $\text{Na}_{1-x}\text{Li}_x\text{Ca}_{0.99}\text{PO}_4:\text{Eu}_{0.01}$ phosphor containing 4 mol% of lithium ($x=4$) is exhibiting better luminescence efficiency when compared with other samples. Moreover, we have done XRD characterization to analyze the possible structural explanation for this. It was found that diffraction patterns of phosphors with and without lithium ions are all the same. Hence the change in the emission intensity is due to the differences of the ionic radii of alkali metal ions. The alkali metal ions of Li^+ , Na^+ and K^+ have the valence electronic configurations of noble gases. The alkali metal ions have ionic radii in the increasing order of $\text{Li}^+ < \text{Na}^+ < \text{K}^+$. The difference in the ionic radii would probably give rise to diversity in the sub lattice structure around the luminescent center ions. This in turn influences the spin–orbit coupling and the crystal field of europium ions. Thus, the relative emission intensity of the phosphors incorporated with lithium is strongly enhanced as the coordination conditions of europium ions are influenced due to the change in distances between $\text{Eu}-\text{O}$ [28,29].

In general, color is represented by means of color coordinates. The chromaticity diagram established by the Commission Internationale de l'Éclairage (CIE) in 1931 is a two dimensional graphical representation of any color perceivable by the human eye on an x – y plot. Hence, in our present work, the chromaticity coordinates of $\text{Na}_{1-x}\text{Li}_x\text{Ca}_{0.99}\text{PO}_4:\text{Eu}_{0.01}$ phosphors sintered in argon atmosphere

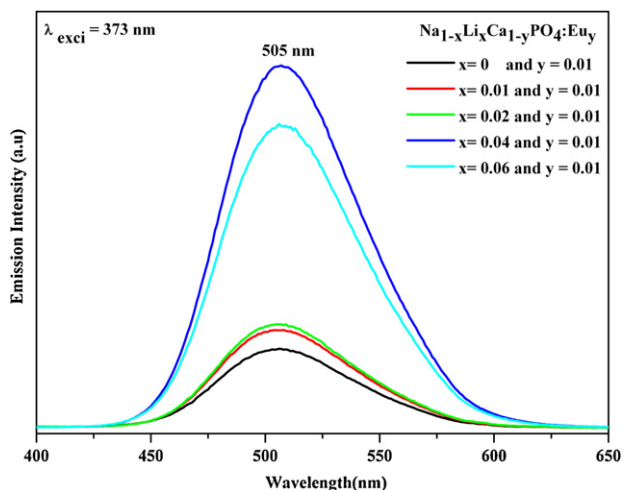


Fig. 7. PL Emission Spectra of $\text{Na}_{1-x}\text{Li}_x\text{Ca}_{0.99}\text{PO}_4:\text{Eu}_{0.01}$ phosphors sintered in argon atmosphere with varying lithium ion concentrations.

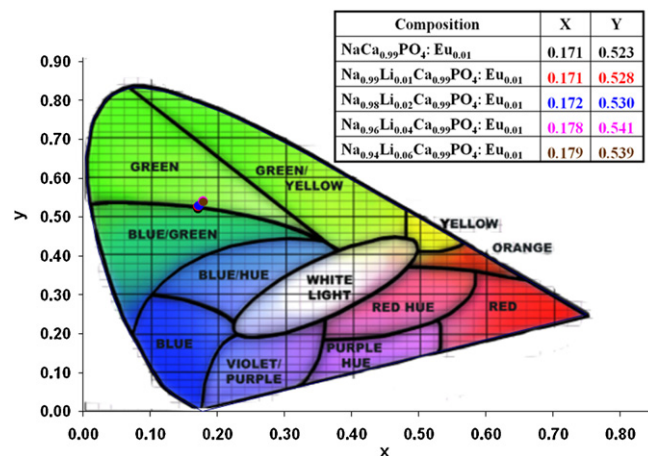


Fig. 8. CIE color coordinates of $\text{Na}_{1-x}\text{Li}_x\text{Ca}_{0.99}\text{PO}_4:\text{Eu}_{0.01}$ phosphors sintered in argon atmosphere. (For interpretation of the references to color in this figure legend, the reader is referred to the web version of this article.)

has been calculated from their corresponding emission spectra and its color coordinates are depicted in Fig. 8.

4. Conclusions

For the first time, we have reported about the reduction phenomenon of Eu^{3+} to Eu^{2+} in NaCaPO_4 compound sintered in non-reducing atmosphere of pure Argon gas. This reduction phenomenon was also explained by using charge compensation model. The un-equivalent substitution of Eu^{3+} for Ca^{2+} creates electrons on $[\text{V}_{\text{Ca}}]'$ vacancies in NaCaPO_4 matrix. The tetrahedral PO_4 anion groups of the compounds probably played a role of electron transfer in the reduction process of Eu^{3+} to Eu^{2+} in non-reducing atmosphere of pure argon. Emission spectral profiles and temperature dependant emission studies revealed that the prepared $\text{NaCaPO}_4:\text{Eu}^{2+}$ phosphors are potential enough for WLEDs and display device applications.

Acknowledgements

This work was supported by the Priority Research Centers Program through the National Research Foundation of Korea funded by the Ministry of Education, Science and Technology (NRF-2010-0029634) and also this work was partially supported by the National Research Foundation of Korea funded by the Korean government (NRF-2010-0023034).

References

- [1] S. Ye, F. Xiao, Y.X. Pan, Y.Y. Ma, Q.Y. Zhang, Mater. Sci. Eng. R 71 (2010) 1–34.
- [2] B. Liu, Y. Wang, J. Zhou, F. Zhang, Z. Wang, J. Appl. Phys. 106 (2009) 053102.
- [3] J.K. Han, G.A. Hirata, J.B. Talbot, J. McKittrick, Mater. Sci. Eng. B 176 (2011) 436–441.
- [4] S. Zhang, Y. Huang, H.J. Seo, J. Electrochem. Soc. 157 (7) (2010) J261–J266.
- [5] Z. Pei, Q. Zeng, Q. Su, J. Phys. Chem. Solids 61 (2000) 9–12.
- [6] M. Peng, Z. Pei, G. Hong, Q. Su, J. Mater. Chem. 13 (2003) 1202–1205.
- [7] G. Gao, S. Reibstein, M. Peng, L. Wondraczek, J. Mater. Chem. 21 (2011) 3156–3161.
- [8] W. Tang, Y. Zheng, Luminescence 25 (2010) 364–366.
- [9] M. Peng, Z. Pei, G. Hong, Q. Su, Chem. Phys. Lett. 371 (2003) 1–6.
- [10] B. Yan, C. Wang, Solid State Sci. 10 (2008) 82–89.
- [11] R.A. Nyquist, R.O. Kagel, Infrared Spectra of Inorganic Compounds ($3800-45\text{ cm}^{-1}$), Academic Press, NY, 1997, p. 232.
- [12] F. Lei, B. Yan, J. Solid State Chem. 181 (2008) 855–862.
- [13] K. Vivekanandan, S. Selvasekarapandian, P. Kolandaivel, M.T. Sebastian, S. Suma, Mater. Chem. Phys. 49 (1997) 204–210.
- [14] Y. Huang, X. Wang, H.S. Lee, E. Cho, K. Jang, Y. Tao, J. Phys. D: Appl. Phys. 40 (2007) 7821–7825.
- [15] R.L. Frost, J. Cejka, M. Weier, Spectrochim. Acta A 65 (2006) 797–801.

- [16] P.D. Belsare, C.P. Joshi, S.V. Moharil, V.K. Kondawar, P.L. Muthal, S.M. Dhopte, J. Alloys Compd. 450 (2008) 468–472.
- [17] C. Qin, Y. Huang, L. Shi, G. Chen, X. Qiao, H.J. Seo, J. Phys. D: Appl. Phys. 42 (2009) 185105.
- [18] Z. Yang, G. Yang, S. Wang, J. Tian, X. Li, Q. Guo, G. Fu, Mater. Lett. 62 (2008) 1884–1886.
- [19] J. Gu, B. Yue, G. Yin, X. Liao, Z. Huang, Y. Yao, Y. Kang, Front. Mater. Sci. Chin. 4 (1) (2010) 90–94.
- [20] J. Qiu, K. Miura, N. Sugimoto, K. Hirao, J. Non-Cryst. Solids 213–214 (1997) 266–270.
- [21] Y. Wang, Z. Zhang, J. Solid State Chem. 182 (2009) 813–820.
- [22] M. Penga, G. Hong, J. Lumin. 127 (2007) 735–740.
- [23] R.D. Shannon, Acta Crystallogr. A 32 (1976) 751–767.
- [24] S. Zhang, X. Wu, Y. Huang, Int. J. Appl. Ceram. Technol., in press, doi:10.1111/j.1744-7402.2010.02541.x.
- [25] S. Shionoy, W.M. Yen, Phosphor Handbook, CRC Press, NY, 1998.
- [26] R. Balakrishnaiah, S.S. Yi, K. Jang, H.S. Lee, Mater. Res. Bull. 46 (2011) 621–626.
- [27] J. Huang, R. Gao, Z. Lu, D. Qian, W. Li, B. Huang, X. He, Opt. Mater. 32 (2010) 857–861.
- [28] R. Ghildiyal, C.H. Hsu, C.H. Lu, Int. J. Appl. Ceram. Technol., in press, doi:10.1111/j.1744-7402.2010.02560.x.
- [29] X. Li, L. Guan, X. Li, Powder Technol. 200 (2010) 12–15.